Advances in Atmospheric Sciences
Impact Factor: 3.158
E-alert
ISSN 0256-1530
CN 11-1925/O4

An Unprecedented Record Low Antarctic Sea-ice Extent during Austral Summer 2022

Jinfei WANG, Hao LUO, Qinghua YANG, Jiping LIU, Lejiang YU, Qian SHI, Bo HAN

Citation: Wang, J. F., H. Luo, Q. H. Yang, J. P. Liu, L. J. Yu, Q. Shi, and B. Han 2022: An Unprecedented Record Low Antarctic Sea-ice Extent during Austral Summer 2022, *Adv. Atmos. Sci.*, In press. doi: 10.1007/s00376-022-2087-1.

View online: https://doi.org/10.1007/s00376-022-2087-1

ADVANCES IN ATMOSPHERIC SCIENCES, VOL. 39, OCTOBER 2022, 1591–1597

• News & Views •

An Unprecedented Record Low Antarctic Sea-ice Extent during Austral Summer 2022

Jinfei WANG[1], Hao LUO[*1], Qinghua YANG[1], Jiping LIU[2], Lejiang YU[3], Qian SHI[1], and Bo HAN[1]

[1]*School of Atmospheric Sciences, Sun Yat-sen University, and Southern Marine Science and Engineering Guangdong Laboratory (Zhuhai), Zhuhai* 519082, *China*

[2]*Department of Atmospheric and Environmental Sciences University at Albany, State University of New York, New York* 12222, *USA*

[3]*Ministry of Natural Resources Key Laboratory for Polar Science, Polar Research Institute of China, Shanghai* 200136, *China*

(Received 24 March 2022; revised 31 March 2022; accepted 6 April 2022)

ABSTRACT

Seasonal minimum Antarctic sea ice extent (SIE) in 2022 hit a new record low since recordkeeping began in 1978 of 1.9 million km^2 on 25 February, 0.17 million km^2 lower than the previous record low set in 2017. Significant negative anomalies in the Bellingshausen/Amundsen Seas, the Weddell Sea, and the western Indian Ocean sector led to the new record minimum. The sea ice budget analysis presented here shows that thermodynamic processes dominate sea ice loss in summer through enhanced poleward heat transport and albedo–temperature feedback. In spring, both dynamic and thermodynamic processes contribute to negative sea ice anomalies. Specifically, dynamic ice loss dominates in the Amundsen Sea as evidenced by sea ice thickness (SIT) change, while positive surface heat fluxes contribute most to sea ice melt in the Weddell Sea.

Key words: Antarctic, record low, sea ice budget, atmospheric circulation

Citation: Wang, J. F., H. Luo, Q. H. Yang, J. P. Liu, L. J. Yu, Q. Shi, and B. Han, 2022: An unprecedented record low Antarctic sea-ice extent during austral summer 2022. *Adv. Atmos. Sci.*, **39**(10), 1591−1597, https://doi.org/10.1007/s00376-022-2087-1.

1. Introduction

Changes in Antarctic sea ice cover can affect heat, moisture, and gas exchanges between the atmosphere and ocean (Raphael, 2003; Kurtz et al., 2011; Søren et al., 2011), freshwater input, ocean circulation (Aagaard and Carmack, 1989; Kirkman and Bitz, 2011; Ferrari et al., 2014), local weather systems, and global climate change (Vihma, 2014; Smith et al., 2017; Ayres and Screen, 2019). Contrary to the rapid decline of the Arctic sea ice extent (SIE) in the context of global warming (Stroeve et al., 2007; Notz and Stroeve, 2016; Serreze and Meier, 2019), Antarctic SIE displays a modest increasing trend of ~1.0% ± 0.5% per decade since late 1978 (Parkinson, 2019), masking significant interannual and regional variations (Liu et al., 2004; Stammerjohn and Maksym, 2016; Yuan et al., 2017; Maksym, 2019). Annual mean Antarctic SIE hit a record high in 2014 (12.8 million km^2) after a long-term increase since 1978 and then plunged to a record low in 2017 (10.7 million km^2). The reasons behind the variability of Antarctic sea ice are complicated, and various mechanisms have been proposed (Hobbs et al., 2016; Maksym, 2019; Eayrs et al., 2021). Seasonal minimum SIE also hit a record low (2.3 million km^2) on 1 March 2017. However, it has been broken after merely five years, as SIE reached 1.9 million km^2 on 25 February 2022. This is the first time SIE has reached below 2 million km^2 since satellite observation began, and this record low is ~30% lower than 1981–2010 climatology (Fig. 1a). This lowest SIE mainly resulted from large negative SIE anomalies in the Bellingshausen/Amundsen Seas, the Weddell Sea, and the western Indian Ocean sector (Fig. 1b).

In a very recent publication, Raphael and Handcock (2022) commented that the new record SIE minimum in austral summer 2022 might have been caused by the early retreat of the ice in August 2021. Here, we examine the relative roles of

* Corresponding author: Hao LUO
Email: luohao25@mail.sysu.edu.cn

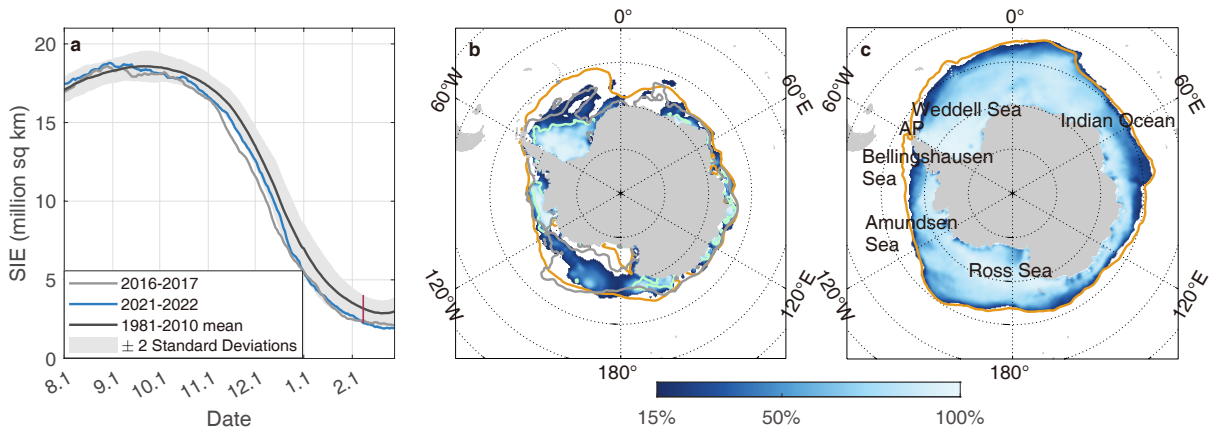

Fig. 1. (a) Time series of Antarctic sea ice extent (SIE) from 1 August to 28 February of the next year during 2016–17 (grey) and 2021–22 (blue), and average SIE based on the period 1981–2010 (black) with two standard deviations (SDs; grey shade). The red vertical line indicates the date (8 February) when 2022 SIE is beyond the range of two SDs of the climatology. (b) Sea ice concentration (SIC) distribution for austral summer (December to February 2022) with an outline of the 30-year (1981–2010) average SIC (orange line), an outline of the minimum SIC on 25 February (cyan line), and an outline of 2016–17 summer average SIC (grey line). The outlines are defined with the 15% contour of SIC. (c) SIC distribution for austral spring (September to November 2021) with an outline of the 30-year (1981–2010) average SIC (orange line).

dynamics and thermodynamics in contributing to the extremely low Antarctic SIE in spring and summer 2022 through a sea ice concentration (SIC) budget analysis.

2. Data and methods

2.1. *Data*

Daily SIC data on a 25-km grid for the period 1979–2022 from the National Snow and Ice Data Center (NSIDC) are used for the sea ice budget analyses. The SIC data are derived from the brightness temperatures measured by the Nimbus-7 Scanning Multichannel Microwave Radiometer and the Defense Meteorological Satellite Program's Special Sensor Microwave/Imager and Special Sensor Microwave Imager/Sounder using the NASA Team algorithm (Cavalieri et al., 1996; Meier et al., 2021). Daily sea ice drift (SID) during 1979–2020 (Tschudi et al., 2019a) and weekly quicklook SID since 2021 (Tschudi et al., 2019b) are also obtained from the NSIDC (ending on 4 February). The SID data are derived by merging data from different sources, including the Advanced Very High Resolution Radiometer, passive microwaves, IABP buoys, and NCEP/NCAR reanalysis. To reduce the uncertainty in the ice drift fields, we smooth the daily ice drift fields with a 7×7 cell square-window filter following Holland and Kimura (2016). Daily SIE data from 1979 to 2022 are based on the NSIDC Sea Ice Index (https://nsidc.org/data/seaice_index). The NASA Ice, Cloud, and land Elevation Satellite-2 (ICESat-2) monthly gridded sea ice freeboard (SIF) data with 25-km resolution from 2018 to 2021 are also used to facilitate the analysis (Petty et al., 2021).

Hourly sea level pressure (SLP), 10-m winds (W10), 2-m air temperature (T2m), surface net shortwave (SW_{net}; positive downwards for all fluxes) and longwave (LW_{net}) radiative fluxes, surface latent heat (H_l), and sensible heat (H_s) fluxes are obtained from the ERA5 reanalysis (ECMWF, 2018). All these variables are retrieved with 0.25°×0.25° resolution and converted to monthly means from September 2021 to February 2022. Anomalies are calculated by removing the seasonal cycle based on the 1981–2010 climatology. ERA5 is the latest climate reanalysis produced by European Centre for Medium-Range Weather Forecasts and has been widely used in previous studies on the Antarctic (e.g., Tetzner et al., 2019; Dong et al., 2020; Zhu et al., 2021).

2.2. *Methodology*

Following the sea ice budget method of Holland and Kwok (2012), sea ice tendency can be decomposed into dynamic ice change and residual change [see Eq. (1)]. This method has been applied in previous studies to diagnose the SIC budget (e.g., Holland and Kimura, 2016; Pope et al., 2017) and validate whether climate models can produce realistic dynamic and thermodynamic contributions of sea ice changes (e.g., Uotila et al., 2014; Lecomte et al., 2016).

$$\frac{\partial C}{\partial t} = -\nabla \cdot (\boldsymbol{u}C) + \text{residual}\,,$$

where C is sea ice concentration and $\boldsymbol{u}$ is sea ice drift. $\partial C/\partial t$ is sea ice tendency and is calculated as the central difference

between one day after and before the specific day. $-\nabla\cdot(\boldsymbol{u}C)$ represents the dynamic processes, which are calculated using the central difference in space and then smoothed using a three-day average. The residual term includes the contributions from the thermodynamic processes and mechanical redistribution. Positive values are connected to increased ice concentration. In this study, we calculate the ratio between the dynamic term and the ice tendency to indicate the residual-induced contributions. Both the ice tendency and the dynamic term are cumulated through spring (September–November; SON) and summer (December–February, until 4 February due to lack of SID; DJF).

3. Results

Since Antarctic sea ice basically melts from September to February, the record low SIE in February is caused by total melting in spring and summer. Figure 1a shows the evolution of SIE in spring 2021 and summer 2022. Apparently, compared to the climatology, sea ice retreated earlier (started from early September), the negative anomalies became larger until mid-November and changed little until mid-December, and SIE dropped quickly exceeding two standard deviations (SDs) of the climatology on 8 February. Compared to 2017, the SIE in 2022 had a delayed recovery in late February, leading to the new record minimum.

Spatially, in austral summer, significant SIE anomalies are located in the western Amundsen Sea, eastern Ross Sea, west of Antarctic Peninsula, northern Weddell Sea, and northwestern Indian Ocean sector (Fig. 1b). It is noteworthy that sea ice in the western Amundsen Sea and the eastern Ross Sea completely disappeared on 25 February, which is also an important feature of the SIC minimum on 1 March 2017. In spring, SIE anomalies are negative in the western Weddell Sea, the Bellingshausen Sea, and the eastern Indian Ocean (Fig. 1c).

Summer SIC anomalies reveal widespread negative anomalies with the largest anomalies in the southwestern Amundsen Sea, southeastern Ross Sea, and the northwestern Weddell Sea, though there are some clustered positive anomalies (Fig. 2a). Sea ice tendency shows a decrease from December to February in most of the Antarctic (Fig. 2b). However, dynamic processes cannot explain the integrated ice tendency (Fig. 2c). Therefore, summer ice loss is dominantly attributed to thermodynamic processes. The SLP field shows a broad low pressure anomaly over the high-latitude Southern Hemisphere with the center in the eastern Ross Sea, leading to a deepening and westward shift of the Amundsen Sea Low (ASL). Induced by the SLP anomalies, westerly winds are intensified between 60°S and 70°S, and there are cyclonic circulations in the Ross Sea and Weddell Sea (Fig. 2e). Consequently, poleward heat transport is enhanced in the Bellingshausen/Amundsen Seas, eastern Weddell Sea, and the western Pacific Ocean, which accelerates sea ice melting (Fig. 2e). In addition, positive net heat flux anomalies are found in the Amundsen Sea and the Weddell Sea, dominated by SW_{net} anomalies, which are consistent with negative SIC anomalies (Fig. 2f). H_l and H_s account for a small proportion of the positive anomalies, while LW_{net} shows few anomalies over the Southern Ocean. As more sea ice is melted in summer, more open water emerges, absorbing more shortwave radiation and lowering surface albedo, thus resulting in more sea ice melting.

In austral spring, SIC also displays circumpolar negative anomalies, with the largest changes in the Weddell Sea, the Bellingshausen Sea, and the eastern Indian Ocean (Fig. 3a). This indicates that summer ice loss as discussed above follows the sea ice melting at an earlier stage. Thus, it is necessary to look at the sea ice budget and atmospheric circulation in spring. Like summer, sea ice tendency in spring also shows an overall decrease, but mostly at the ice edge zone (Fig. 3b). Dynamic processes dominate the spring tendency due to strong sea ice drift (Fig. 3c), giving rise to SIC decline in the inner ice pack areas like the Amundsen Sea, Ross Sea, and the Weddell Sea, and SIC increases at the ice edge. Northward ice motion pushes more ice to the lower latitudes and increases melting, especially in the Amundsen Sea and the Ross Sea, providing a chance for total ice melting there in summer. Besides, from Fig. 3c we can also see that the rest of the tendency should be represented by the residual term (thermodynamic processes). Therefore, we attribute spring tendency to the combined impacts of dynamic and thermodynamic processes. The SLP fields show below-normal SLP in the eastern Amundsen Sea that is much stronger than that of summer (Fig. 3d), leading to strong cyclonic winds. Northerly winds and southward heat transport happen in the Weddell Sea and the Bellingshausen Sea, while southerly winds and northward heat transport happen in the Amundsen Sea and eastern Ross Sea (Fig. 3e). Positive net heat flux anomalies appear in the Weddell Sea, caused by SW_{net}, H_l, and H_s anomalies (Fig. 3f).

Changes in SIT have a preconditioning role in the rate of sea ice retreat. As demonstrated by ICESat-2 SIF, sea ice in spring 2021 was much thinner along the coast of the Amundsen Sea compared with SIF during 2018–20, and it was accompanied with strong northward dispersion of sea ice, leading to more open water (Fig. 4). This provides a favorable precondition for summer sea ice melting there and might be related to the record temperatures of the Southern Ocean in 2021 (Cheng et al., 2022).

4. Conclusions and discussion

Our study gives a thorough description of the features in the Antarctic SIE minimum in February 2022. SIE reached a

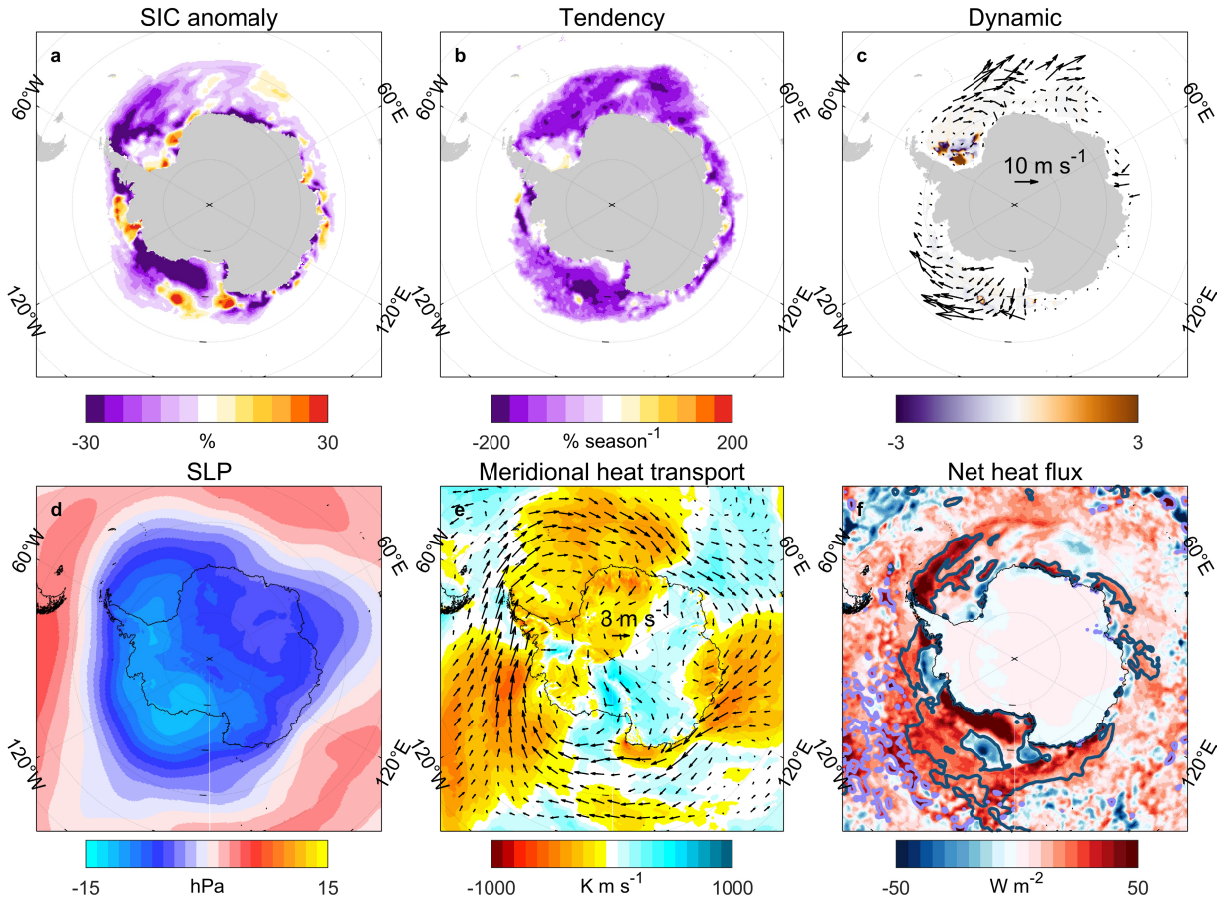

Fig. 2. (a) SIC anomalies for austral summer based on 1981–2010 average SIC (units: %). (b) SIC tendency ($\partial C/\partial t$) from 1 December to 4 February (units: % season^{-1}). (c) The ratio of the dynamic contributions [$-\nabla\cdot(\boldsymbol{u}C)$] to tendency from 1 December to 4 February. The vectors represent seasonal average sea ice drift. (d) Anomalies of sea level pressure (units: hPa). (e) Anomalies of meridional heat transport (units: K m s^{-1}) and 10-m wind (units: m s^{-1}). (f) Anomalies of surface net heat fluxes (shaded), net shortwave radiation fluxes of 20 W m^{-2} (dark blue contour), and the sum of net sensible and latent heat fluxes of 20 W m^{-2} (purple contour) (units: W m^{-2}).

new record low since recordkeeping began in 1978 of 1.9 million km^2 on 25 February, 0.17 million km^2 lower than the previous record low set in 2017. One reason for this is that the Antarctic sea ice retreated earlier than normal, starting from early September of 2021. The negative anomalies became larger until mid-November, and then sea ice exhibited a steadily decreasing rate until mid-December of 2021 and dropped quickly, exceeding two standard deviations (SDs) of the climatology, on 8 February 2022. Significant negative SIC anomalies in summer were located in the western Amundsen Sea, eastern Ross Sea, west of Antarctic Peninsula, northern Weddell Sea, and northwestern Indian Ocean sector, while spring SIC anomalies were negative in most sectors, basically confined in the western Weddell Sea, the Bellingshausen Sea, and the eastern Indian Ocean. We analyze the sea ice budget over the melting seasons and connect the atmospheric circulation with them. In summer, thermodynamic processes dominate the sea ice melting through poleward heat transport anomalies in the Bellingshausen/Amundsen Seas, eastern Weddell Sea, and the western Pacific Ocean and positive net shortwave radiation anomalies with albedo–temperature feedback. In spring, dynamic and thermodynamic processes contribute to sea ice tendency together. Dynamic ice loss exists in the Amundsen Sea where northward ice motion pushes more ice to the lower latitudes and increases melting, especially in the Amundsen Sea and the Ross Sea. Thermodynamic contributions including poleward heat transport, shortwave radiation, and sensible and latent heat flux anomalies melt sea ice in the Weddell Sea. Meanwhile, thinner sea ice freeboard along the coast of the Amundsen Sea is also critical to the summer melting. All these atmospheric impacts originate from the intensity and position of ASL and ocean warming, proving the deductions made by Raphael and Handcock (2022).

According to the NOAA Climate Prediction Center, the monthly Antarctic Oscillation (AAO) index and Oceanic Niño Index show that the new record Antarctic SIE minimum happened during a combination of positive Southern Annular Mode (SAM) and La Niña. Both of these modes lead to a deepened ASL (Yu et al., 2015; Fogt and Marshall, 2020). Fogt et al. (2011) revealed that when a La Niña (El Niño) is concurrent with a positive (negative) SAM, the impact of ENSO is signif-

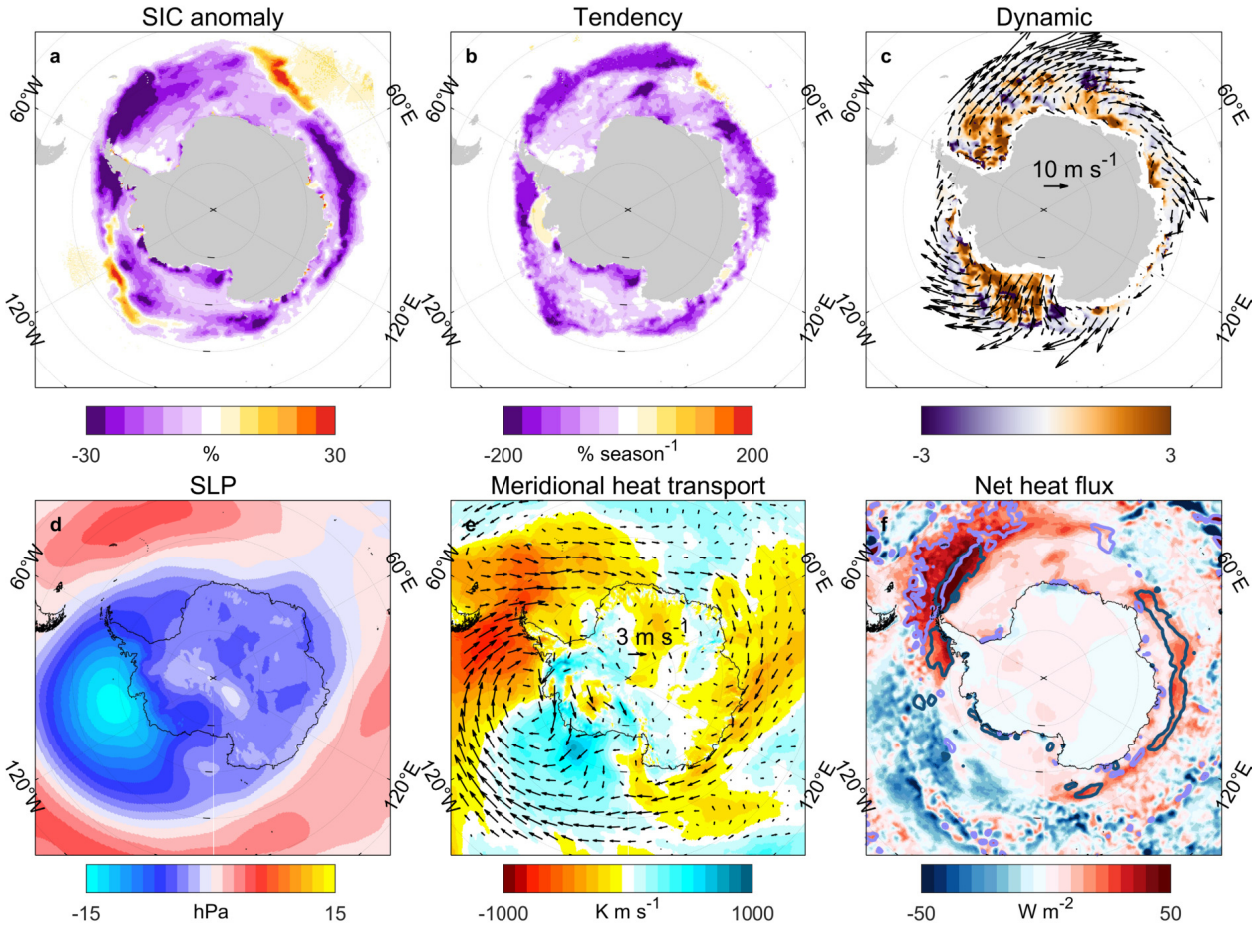

Fig. 3. Same as Fig. 2 but for austral spring (September–November; SON).

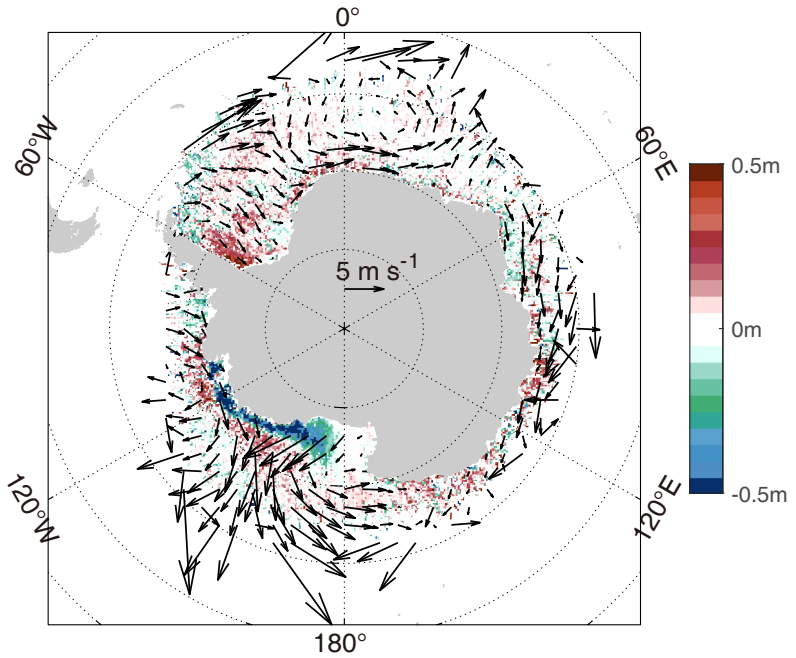

Fig. 4. Sea ice freeboard anomalies (shading) and sea ice motion anomalies (vectors) in spring 2021 based on average spring values during 2018–20.

icant on South Pacific atmospheric circulation. Stammerjohn et al. (2008) investigated the relationship between these combined impacts and the sea ice retreat/advance and showed a similar result to the in-phase condition in Fogt et al. (2011), with significant ice responses, particularly in the western Antarctic Peninsula and the southern Bellingshausen Sea. In addition, the Indian Ocean Dipole, Interdecadal Pacific Oscillation, and the Atlantic Multidecadal Oscillation are all important factors contributing to Antarctic sea ice decline in spring 2016 (Eayrs et al., 2021). Therefore, impacts of tropical variability and large-scale climate modes should be further studied.

Besides, examining the physical cause of the difference of the SIC distribution between 2016–17 and 2021–22 can help us understand the physical causes of the interannual variability of the Antarctic sea ice. Figure 1b reveals that the 2017 summer SIC pattern shows a few differences in the eastern Ross Sea, Bellingshausen Sea, and the northern Weddell Sea compared with the 2022 summer. More sea ice is melted in the Weddell Sea rather than in the Ross Sea in 2017. By comparing the sea ice budgets and atmospheric circulations of the two events (not shown), we find a different budget result and opposite SLP anomalies and thus suggest that the underlying mechanisms might be different in these two recent record low SIE events. Detailed and comprehensive investigations are required to further verify this deduction.

Acknowledgements. The authors wish to thank the editor and two anonymous reviewers for their very helpful comments and suggestions. This is a contribution to the Year of Polar Prediction (YOPP), a flagship activity of the Polar Prediction Project (PPP), initiated by the World Weather Research Programme (WWRP) of the World Meteorological Organisation (WMO). We acknowledge the WMO WWRP for its role in coordinating this international research activity. This study is supported by the National Natural Science Foundation of China (Grant Nos. 41941009, 41922044, and 42006191), the Guangdong Basic and Applied Basic Research Foundation (Grant No. 2020B1515020025), and the Fundamental Research Funds for the Central Universities (Grant No. 19lgzd07), the Norges Forskningsråd (Grant no. 328886).

REFERENCES

Aagaard, K., and E. C. Carmack, 1989: The role of sea ice and other fresh water in the Arctic circulation. *J. Geophys. Res.*, **94**, 14 485–14 498, https://doi.org/10.1029/JC094iC10p14485.

Ayres, H. C., and J. A. Screen, 2019: Multimodel analysis of the atmospheric response to Antarctic sea ice loss at quadrupled CO_2. *Geophys. Res. Lett.*, **46**, 9861–9869, https://doi.org/10.1029/2019GL083653.

Cavalieri, D. J., C. L. Parkinson, P. Gloersen, and H. J. Zwally, 1996: Updated yearly. Sea ice concentrations from nimbus-7 SMMR and DMSP SSM/I-SSMIS passive microwave data, Version 1. Boulder, Colorado USA. NASA National Snow and Ice Data Center Distributed Active Archive Center. Available from http://dx.doi.org/10.5067/8GQ8LZQVL0VL. https://doi.org/10.5067/8GQ8LZQVL0VL.

Cheng, L. J., and Coauthors, 2022: Another record: Ocean warming continues through 2021 despite La Niña conditions. *Adv. Atmos. Sci.*, **39**, 373–385, https://doi.org/10.1007/s00376-022-1461-3.

Dong, X., Y. T. Wang, S. G. Hou, M. H. Ding, B. L. Yin, and Y. L. Zhang, 2020: Robustness of the recent global atmospheric reanalyses for Antarctic near-surface wind speed climatology. *J. Climate*, **33**, 4027–4043, https://doi.org/10.1175/JCLI-D-19-0648.1.

Eayrs, C., X. C. Li, M. N. Raphael, and D. M. Holland, 2021: Rapid decline in Antarctic sea ice in recent years hints at future change. *Nature Geoscience*, **14**, 460–464, https://doi.org/10.1038/s41561-021-00768-3.

ECMWF, 2018: ERA5 hourly data on single levels from 1979 to present. Available online from https://cds.climate.copernicus.eu/cdsapp#!/dataset/reanalysis-era5-single-levels?tab=overview.

Ferrari, R., M. F. Jansen, J. F. Adkins, A. Burke, A. L. Stewart, and A. F. Thompson, 2014: Antarctic sea ice control on ocean circulation in present and glacial climates. *Proceedings of the National Academy of Sciences of the United States of America*, **111**, 8753–8758, https://doi.org/10.1073/pnas.1323922111.

Fogt, R. L., and G. J. Marshall, 2020: The southern annular mode: Variability, trends, and climate impacts across the southern hemisphere. *WIREs Climate Change*, **11**, e652, https://doi.org/10.1002/wcc.652.

Fogt, R. L., D. H. Bromwich, and K. M. Hines, 2011: Understanding the SAM influence on the South Pacific ENSO teleconnection. *Climate Dyn.*, **36**, 1555–1576, https://doi.org/10.1007/s00382-010-0905-0.

Hobbs, W. R., R. Massom, S. Stammerjohn, P. Reid, G. Williams, and W. Meier, 2016: A review of recent changes in Southern Ocean sea ice, their drivers and forcings. *Global and Planetary Change*, **143**, 228–250, https://doi.org/10.1016/j.gloplacha.2016.06.008.

Holland, P. R., and R. Kwok, 2012: Wind-driven trends in Antarctic sea-ice drift. *Nature Geoscience*, **5**, 872–875, https://doi.org/10.1038/ngeo1627.

Holland, P. R., and N. Kimura, 2016: Observed concentration budgets of arctic and Antarctic sea ice. *J. Climate*, **29**, 5241–5249, https://doi.org/10.1175/JCLI-D-16-0121.1.

Kirkman, C. H., and C. M. Bitz, 2011: The effect of the sea ice freshwater flux on southern ocean temperatures in CCSM3: Deep-ocean warming and delayed surface warming. *J. Climate*, **24**, 2224–2237, https://doi.org/10.1175/2010JCLI3625.1.

Kurtz, N. T., T. Markus, S. L. Farrell, D. L. Worthen, and L. N. Boisvert, 2011: Observations of recent Arctic sea ice volume loss and its impact on ocean-atmosphere energy exchange and ice production. *J. Geophys. Res.*, **116**, C04015, https://doi.org/10.1029/2010JC006235.

Lecomte, O., H. Goosse, T. Fichefet, P. R. Holland, P. Uotila, V. Zunz, and N. Kimura, 2016: Impact of surface wind biases on the Antarctic sea ice concentration budget in climate models. *Ocean Modelling*, **105**, 60–70, https://doi.org/10.1016/j.ocemod.2016.08.

001.
Liu, J. P., J. A. Curry, and D. G. Martinson, 2004: Interpretation of recent Antarctic sea ice variability. *Geophys. Res. Lett.*, **31**, L02205, https://doi.org/10.1029/2003GL018732.
Maksym, T., 2019: Arctic and Antarctic sea ice change: Contrasts, commonalities, and causes. *Annual Review of Marine Science*, **11**, 187–213, https://doi.org/10.1146/annurev-marine-010816-060610.
Meier, W. N., J. S. Stewart, H. Wilcox, M. A. Hardman, and D. J. Scott, 2021: Near-Real-Time DMSP SSMIS daily polar gridded sea ice concentrations, Version 2. Boulder, Colorado USA. NASA National Snow and Ice Data Center Distributed Active Archive Center. Available from https://doi.org/10.5067/YTTHO2FJQ97K.
Notz, D., and J. Stroeve, 2016: Observed Arctic sea-ice loss directly follows anthropogenic CO_2 emission. *Science*, **354**, 747–750, https://doi.org/10.1126/science.aag2345.
Parkinson, C. L., 2019: A 40-y record reveals gradual Antarctic sea ice increases followed by decreases at rates far exceeding the rates seen in the Arctic. *Proceedings of the National Academy of Sciences of the United States of America*, **116**, 14 414–14 423, https://doi.org/10.1073/pnas.1906556116.
Petty, A. A., R. Kwok, M. Bagnardi, A. Ivanoff, N. Kurtz, J. Lee, J. Wimert, and D. Hancock, 2021. ATLAS/ICESat-2 L3B daily and monthly gridded sea ice freeboard, Version 3. Boulder, Colorado USA. NASA National Snow and Ice Data Center Distributed Active Archive Center. Available from https://nsidc.org/data/atl20/versions/3.
Pope, J. O., P. R. Holland, A. Orr, G. J. Marshall, and T. Phillips, 2017: The impacts of El Niño on the observed sea ice budget of West Antarctica. *Geophys. Res. Lett.*, **44**, 6200–6208, https://doi.org/10.1002/2017GL073414.
Raphael, M. N., 2003: Impact of observed sea - ice concentration on the Southern Hemisphere extratropical atmospheric circulation in summer. *J. Geophys. Res.*, **108**, 4687, https://doi.org/10.1029/2002JD003308.
Raphael, M. N., and M. S. Handcock, 2022: A new record minimum for Antarctic sea ice. *Nature Reviews Earth & Environment*, https://doi.org/10.1038/s43017-022-00281-0.
Serreze, M. C., and W. N. Meier, 2019: The Arctic's sea ice cover: Trends, variability, predictability, and comparisons to the Antarctic. *Annals of the New York Academy of Sciences*, **1436**, 36–53, https://doi.org/10.1111/nyas.13856.
Smith, D. M., N. J. Dunstone, A. A. Scaife, E. K. Fiedler, D. Copsey, and S. C. Hardiman, 2017: Atmospheric response to arctic and Antarctic sea ice: The importance of ocean–atmosphere coupling and the background state. *J. Climate*, **30**, 4547–4565, https://doi.org/10.1175/JCLI-D-16-0564.1.
Søren, R., and Coauthors, 2011: Sea ice contribution to the air–sea CO_2 exchange in the Arctic and Southern Oceans. *Tellus B: Chemical and Physical Meteorology*, **63**, 823–830, https://doi.org/10.1111/j.1600-0889.2011.00571.x.
Stammerjohn, S., and T. Maksym, 2016: Gaining (and losing) Antarctic sea ice: Variability, trends and mechanisms. *Sea Ice*, 3rd ed., D. N. Thomas, Ed., John Wiley & Sons, Ltd., 261–289, https://doi.org/10.1002/9781118778371.ch10.
Stammerjohn, S. E., D. G. Martinson, R. C. Smith, X. Yuan, and D. Rind, 2008: Trends in Antarctic annual sea ice retreat and advance and their relation to El Niño–Southern Oscillation and Southern Annular Mode variability. *J. Geophys. Res.*, **113**, C03S90, https://doi.org/10.1029/2007JC004269.
Stroeve, J., M. M. Holland, W. Meier, T. Scambos, and M. Serreze, 2007: Arctic sea ice decline: Faster than forecast. *Geophys. Res. Lett.*, **34**, L09501, https://doi.org/10.1029/2007GL029703.
Tetzner, D., E. Thomas, and C. Allen, 2019: A validation of ERA5 reanalysis data in the Southern Antarctic peninsula—Ellsworth land region, and its implications for ice core studies. *Geosciences*, **9**, 289, https://doi.org/10.3390/geosciences9070289.
Tschudi, M., W. N. Meier, J. S. Stewart, C. Fowler, and J. Maslanik, 2019a: Polar pathfinder daily 25 km EASE-Grid sea ice motion vectors, Version 4. Boulder, Colorado USA. NASA National Snow and Ice Data Center Distributed Active Archive Center. Available from https://doi.org/10.5067/INAWUWO7QH7B.
Tschudi, M., W. N. Meier, and J. S. Stewart, 2019b: Quicklook arctic weekly EASE-grid sea ice motion vectors, Version 1. Boulder, Colorado USA. NASA National Snow and Ice Data Center Distributed Active Archive Center. Available from https://nsidc.org/data/NSIDC-0748/versions/1.
Uotila, P., P. R. Holland, T. Vihma, S. J. Marsland, and N. Kimura, 2014: Is realistic Antarctic sea-ice extent in climate models the result of excessive ice drift. *Ocean Modelling*, **79**, 33–42, https://doi.org/10.1016/j.ocemod.2014.04.004.
Vihma, T., 2014: Effects of arctic sea ice decline on weather and climate: A review. *Surveys in Geophysics*, **35**, 1175–1214, https://doi.org/10.1007/s10712-014-9284-0.
Yu, J.-Y., H. Paek, E. S. Saltzman, and T. Lee, 2015: The early 1990s change in ENSO–PSA–SAM relationships and its impact on southern hemisphere climate. *J. Climate*, **28**, 9393–9408, https://doi.org/10.1175/JCLI-D-15-0335.1.
Yuan, N. M., M. H. Ding, J. Ludescher, and A. Bunde, 2017: Increase of the Antarctic sea ice extent is highly significant only in the Ross Sea. *Scientific Reports*, **7**, 41096, https://doi.org/10.1038/srep41096.
Zhu, J. P., A. H. Xie, X. Qin, Y. T. Wang, B. Xu, and Y. C. Wang, 2021: An assessment of ERA5 reanalysis for Antarctic near-surface air temperature. *Atmosphere*, **12**, 217, https://doi.org/10.3390/atmos12020217.